A Digital Twin Ocean: Can we improve Coastal Ocean Forecasts using targeted Marine Autonomy?

Dale Partridge[1,5,*], Deep Banerjee[1,5], David Ford[2], Ke Wang[3,4], Jozef Skakala[1,5], Juliane Wihsgott[1], Prathyush P Menon[4], Susan Kay[1,2], Daniel Clewley[1,5], Andrea Rochner[2], Emma Sullivan[1,5], and Matthew Palmer[1]

[1]Plymouth Marine Laboratory, Plymouth, PL1 2LP, UK

[2]Met Office, Exeter, EX1 3PB, UK

[3]Shanghai Jiao Tong University, Shanghai, 200240, China

[4]University of Exeter, Exeter, EX4 4PY, UK

[5]National Centre for Earth Observation, Leicester, LE4 5SP, UK

[*]Corresponding author: Dale Partridge, dapa@pml.ac.uk

Abstract. This study outlines the development and testing of a Digital Twin Ocean (DTO) framework, aimed at improving coastal ocean forecasts through the use of autonomous underwater gliders. A fleet of gliders were deployed in the western English Channel during August-September 2024 to collect measurements of temperature, salinity, chlorophyll and oxygen, aiming to track the movement of the harmful algal bloom *Karenia mikimotoi*. Measurements were assimilated into a very high resolution ($1.5km$) numerical forecast model, with an implementation of biogeochemistry data assimilation for this purpose. The model forecast was then used by a probabilistic uncertainty model to plan a series of waypoints to navigate the glider fleet towards features of interest. By utilising a continuous feedback loop of measurement, prediction, guidance, and refinement a system with real time coupling between the real ocean environment and its digital counterpart has been established.

Building upon a prior pilot study of ~~Ford et al. (2022)~~Ford et al. (2022), this work improves every element of the system to ~~addresses~~ address several limitations of the prior configuration. Whilst a bloom was present in the wider area, measurements and modeling suggest it didn't enter the glider operation zone. Despite this and other operational challenges the mission clearly demonstrates the benefits of such a system. The ability to simultaneously track multiple features of interest, namely chlorophyll ~~and oxygen~~maxima and oxygen minima, would not have been possible with a single glider resulting in significant benefits to the system. Furthermore, the improvement to biogeochemical forecasting has been demonstrated through a series of post mission experiments, highlighting the advantages of high temporal resolution observations and increased spatial resolution of the model.

1 Introduction

Digital twins of the ocean (DTO) are emerging as a key area of marine science research (e.g. ~~Tzachor et al. (2023)~~(Tzachor et al., 2023)), reflected by a range of international activities including the UN Ocean Decade programme Digital Twin of the Ocean (DiTTO, https://ditto-oceandecade.org/) and the European Digital Twin of the Ocean (European DTO, https://digitaltwinocean.mercator-ocean.eu/). DTOs are often understood as digital replicas of the real-world ocean, where information flows in both directions, between the real and virtual, or digital twin. This two-way flow is typically used to allow near real-time decision making purposes in a highly changeable environment, where adaptive monitoring and data delivery that continually updates and improves the digital twin is beneficial ~~Tzachor et al. (2023). DTOs have therefore essential applicability within marine autonomy Ford et al. (2022), allowing~~ (Tzachor et al., 2023). The coastal ocean region is vital to communities around the world, with fisheries and tourism amongst the industries that rely on them. Therefore the ability to accurately replicate these zones through DTOs has essential real world applicability and impact. A key component to DTOs is a level of marine autonomy (Ford et al., 2022), which allow for targeted adjustments to ~~focus on~~ regions and periods of observational interest ~~by~~ through navigating marine autonomous systems (MAS) to those areas. ~~Using such~~ In-situ observations of the ocean are difficult and costly to obtain, with the potential to miss vital information in an ever changing environment. Using targeted MAS offers opportunities to reduce the cost and environmental footprint of observational science by making our observations more efficient ~~and~~ through the use of low-carbon autonomous platforms, such as ocean gliders ~~(Testor et al. (2019)).~~ (Testor et al., 2019). Whilst DTO capability in marine autonomy ~~has already been demonstrated in~~ is still in its infancy, there have been demonstrations of their effectiveness for marine physics applications ~~(Lee et al. (2022); Raza et al. (2022); Buck et al. (2024))~~ (Lee et al., 2022; Raza et al., 2 and to some degree in marine biogeochemistry ~~Ford et al. (2022)~~(Ford et al., 2022; Halvorsen et al., 2026).

More specifically, the study of ~~Ford et al. (2022)~~ Ford et al. (2022) applied a DTO approach to a single glider-based observational mission to track the onset of phytoplankton blooms in the wider coastal region of the western English Channel. The use of gliders within this DTO was essential, as the spatial and temporal resolution with which a glider is capable of observing in a highly dynamical coastal environment is unprecedented. That DTO design was based on assimilating glider data alongside satellite and other in situ data in near-real time into a modified version of the Met Office's operational North-West European Shelf (NWES) forecasting system (e.g. O'Dea et al. (2017); King et al. (2018); Skákala et al. (2018); Skákala et al. (2021)). This provided 2-day forecasts to an independent path-planning machine learning (ML) module that produced future navigational waypoints for the glider to optimise the probability of observing and later predicting a phytoplankton bloom. That DTO system thus provided the glider with full autonomy[1], guided by the AI decision-making process using the information cycled between all available components in real time. The study of ~~Ford et al. (2022) demonstrated the clear~~ Ford et al. (2022) demonstrated the benefits of a fully automated and adaptive observing system. The study also revealed several limitations with the approach taken, which included: (i) identified biases between different observational sources (i.e. satellite and glider) used in the data assimilation, (ii) a relatively coarse spatial horizontal resolution (7 km) of the operational model, which was

---

[1] A human pilot provided oversight for regulatory purposes

too far from the horizontal spatial scales of glider daily operations given they typically travel about 1.2 km/h, and (iii) the limitation of a single glider, targeting a single feature of interest and constrained to a small operational area which constrained the range of unknowns that we could feasibly address within such a dynamic and spatially heterogeneous environment. Further demonstration of the limitations of coarse resolution is provided in Section 3.3.

In this work we substantially improve upon the design of ~~Ford et al. (2022)~~ Ford et al. (2022) by addressing the three issues highlighted above and deliver a full DTO demonstrator in a dynamic coastal system. The focus for our DTO demonstrator was a re-occurring bloom of a toxic phytoplankton species, *Karenia mikimotoi*, in the western English Channel ~~Barnes et al. (2015)~~ (Barnes et al., 2015). The toxins released by *Karenia mikimotoi* are known to be able to kill fish ~~Tangen (1977); Silke et al. (2005); Satake e~~ (Tangen, 1977; Silke et al., 2005; Satake et al., 2005), and have other possible side-effects such as de-oxygenation or even hypoxia and reduced irradiance. The Karenia bloom has been repeatedly detected within the western English Channel region in late Summer-early Autumn ~~Barnes et al. (2015)~~(Barnes et al., 2015), and regional satellite-based detection capability has been developed to monitor its onset ~~Shutler et al. (2012)~~(Shutler et al., 2012). The highly dynamic nature and short time scales associated with such blooms make this an ideal but challenging test for our near real-time DTO approach. The glider sensors can detect total chlorophyll-a concentrations (in mg/m^3) obtained from fluorescence measurements. Such measurements however, cannot currently be unambiguously related to Karenia species biomass, despite chlorophyll-a concentrations being commonly used to provide an indication for total phytoplankton biomass. So while this can provide a valuable indicator related to Karenia blooms, complementary information is beneficial to provide an early warning system based on satellite or in situ fluorescence data alone. Furthermore, substantial phytoplankton blooms occurring in stratified relatively shallow waters can lead to excess microbial oxygen consumption, during remineralization of sinking matter near the sea bottom, potentially decreasing dissolved oxygen to harmful levels. This along with successful glider based studies investigating dissolved oxygen dynamics in similarly energetic shelf seas ~~Williams et al. (2022, 2024)~~ (Williams et al., 2022, 2024) motivated us to include dissolved oxygen concentration as an additional key target observation pursued by the DTO.

The DTO presented here aimed to ~~track and predict Karenia blooms and assoiated deoxygenation~~ test the system capability to track areas of high chlorophyll and low oxygen over 2-months during the August-September 2024 period, with the hope of capturing a Karenia bloom and associated deoxygenation. It was based on a finer spatial resolution model ($1.5km$) compared to ~~Ford et al. (2022)~~Ford et al. (2022), utilized a fleet of three gliders and implemented a more advanced path planning methodology. The $1.5km$ spatial resolution system for the NWES, even though run operationally for marine physics ~~Tonani et al. (2019)~~ (Tonani et al., 2019), has so far not been applied with marine biogeochemistry with data assimilation, so this is an entirely new development and major advance in shelf sea ecosystem modelling that is delivered within this DTO. The fleet of gliders was optimized for complementary purposes, i.e. to simultaneously track phytoplankton maxima and near seabed dissolved oxygen minima, resolving their temporal and spatial variability. This manuscript ~~is one of a series of papers delivering a~~ outlines a proof of concept for the deployment of a fully autonomous, coordinated, fleet of gliders capable of adaptively tracking multiple interconnected processes in a highly dynamical coastal environment~~, including Mansfield et al. (2025) which focuses on data~~

~~architecture and the pipelines that made this work possible. This manuscript focuses on the impact~~. The design of the DTO is outlined in Section 2, followed by a series of post-mission experiments to analyse the impact of glider assimilation (Sec. 3.2) and resolution (Sec. 3.3) on the numerical forecasting component ~~, demonstrating clear benefits from using a higher-spatial resolution model for this purpose in conjunction with high temporal glider measurement. Finally, we summarize the important new lessons learned by this novel development and propose future directions of research in this area~~before discussing the effect on path planning in Section 3.4. As part of the development of this system, a set of data architecture and pipelines were created to make this and future work possible, which is discussed in Mansfield et al. (2025).

2 Modelling System

2.1 Digital Twin Design

The digital twin used in this study is a cyclical system of observation-prediction-navigation, shown schematically below:

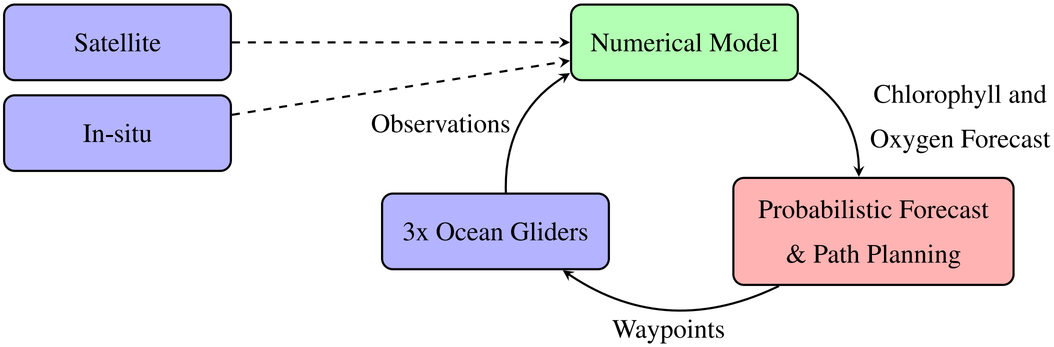

Scheme 1: Cyclical digital twin ocean design

Up to 3 ocean gliders collect high-resolution depth profiles of temperature, salinity, chlorophyll and dissolved oxygen which are transmitted and received whilst the gliders are at the surface. These measurements, along with satellite observations of surface chlorophyll, temperature, and sea level anomaly, and other sources of in situ temperature and salinity observations, are assimilated daily into a numerical model which then produces a multi-day forecast. That forecast informs ~~an AI derived~~ a probabilistic forecast and path planning algorithm to navigate the gliders ~~on~~ during the subsequent 24-48 hours. The various operating domains are shown in Figure 1.

2.2 Observing platforms

2.2.1 Ocean Gliders

As part of the mission, three shallow-water-rated, buoyancy driven Teledyne Webb Slocum G2 ocean gliders (units 480, 481, and 482) were deployed from the Western Channel Observatory's L4 station on 6 August 2024. Each glider was equipped with a Sea-Bird GPCTD sensor, an Aanderaa oxygen optode, and a SeaOWL fluorometer to collect high-resolution vertical profiles

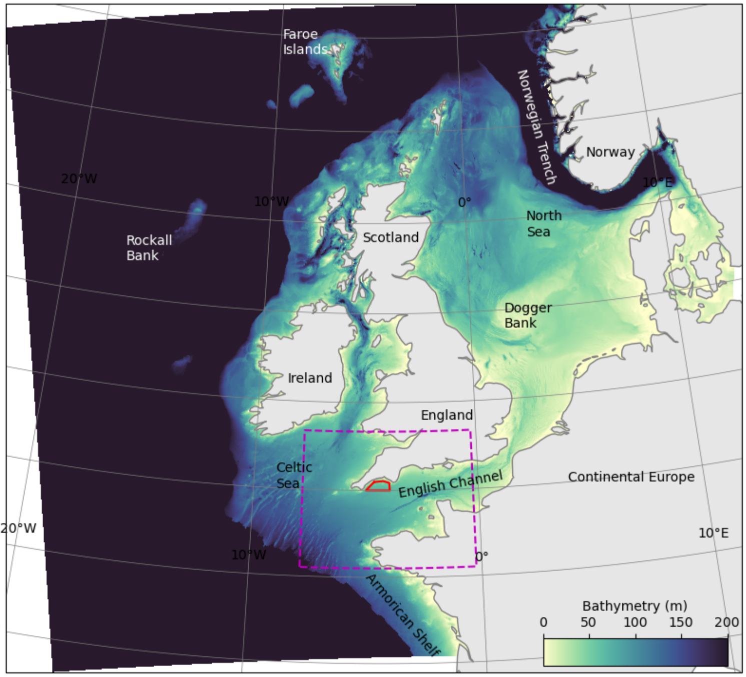

Figure 1. Bathymetry of AMM15 domain area used for the numerical model, showing the extracted region used in the probabilistic forecast (magenta dashed) and the glider operational zone (red)

	Unit 480/481/482
Platform type	Slocum G2, 200 m shallow rated
Sensor 1 (sampling freq)	Seabird GPCTD(1Hz)
Sensor 2 (sampling freq)	SeaOWL fluorometer (1Hz)
Sensor 3 (sampling freq)	Aanderaa Oxygen Optode (0.5Hz)

Table 1. Platform type, sensor models, and sampling frequencies for each Slocum G2 glider deployed during the experiment. The oxygen optode on unit 482 was not operational.

of temperature, salinity, dissolved oxygen, and chlorophyll-a fluorescence. Sensor models, sampling frequencies, and platform details for each glider are summarised in Table 1.

The dissolved oxygen optode connection on 482 malfunctioned during deployment, ~~which prevented~~ preventing the collection of any dissolved oxygen measurements from this vehicle, while the other two gliders were equipped with functioning oxygen optodes . Throughout the campaign, dive and climb profile data were transmitted ashore every six hours at full resolution (1 Hz or 0.5 Hz, depending on the sensor). Given typical vertical speeds of approximately 0.1 m/s, this corresponds to a vertical resolution of approximately 0.1–0.2 m. Successive transmitted vertical profiles were typically separated by approximately 3–5 km horizontally, depending on ambient currents and vehicle speed.

Following deployment, the gliders were manually piloted by human operators for 10 days, after which the autonomous path-planning algorithm produced the waypoints to navigate the vehicles depending on their respective tasks. During the manual pilot period gliders crossed paths several times, sampling the same areas to calibrate the sensors and reduce observational uncertainty. Handover between the path-planning and navigation of gliders was tested and performed under continued human supervision to ensure the safety of the gliders and other sea users and traffic.

Near-real-time (NRT) processing included the application of manufacturer calibrations and corrections for thermal lag. A correction for photochemical quenching was implemented on 30 August 2024, prior to this, daytime Chl-a data were flagged as bad. NRT quality control was managed using adapted Argo processing routines ~~Wong et al. (2023); Schmechtig et al. (2023)~~ (Wong et al., 2023; Schmechtig et al., 2023). In addition, ~~alongside~~ concurrent inherent optical property measurements were used as independent reference to support manual calibration of ~~glider~~ glider-derived Chl-a data, although this was not integrated into the automated processing chain. A simplified approach was attempted to account for oxygen optode response time effects; however, this proved difficult to implement robustly due to the slow optode response. Appropriately corrected and flagged data were made available via an ERDDAP server to support daily assimilation and facilitate ongoing model–data integration.

Following recovery of the gliders, full delayed-mode data processing was conducted using established oceanographic correction methods ~~(Garau et al. (2011); Bittig et al. (2014)), applying both factory calibrationsand~~ (Garau et al., 2011; Bittig et al., 2014) . This included corrections for pressure offset, clock drift, vehicle navigation and application of factory calibrations. We further corrected conductivity data for thermal inertia effects (Garau et al., 2011) , and dissolved oxygen data were corrected for optode response time effects and associated hysteresis following Bittig et al. (2014). Any remaining offsets were assessed through cross-validation against concurrent observations.

2.2.2 Satellite

The Ocean Land Colour Instrument (OLCI), carried onboard the Copernicus Sentinel 3A and Sentinel 3B satellites was used to calculate surface chlorophyll concentration. Data was downloaded from ESA at Level 1 and the Polymer software for atmospheric correction ~~(Steinmetz et al. (2011))~~ (Steinmetz et al., 2011) was used to produce remote sensing reflectance, with the IDEPIX plugin to the SNAP software used to identify and mask out clouds and cloud shadow. Chlorophyll was calculated from the remote sensing reflectance using the OC5CI algorithm. This is a combined algorithm as the OCI algorithm performs better in clear water (case-1), which corresponds to chlorophyll below $0.1\ mg/m^3$, whilst OC5 is better in turbid waters (case-2), where chlorophyll is above $0.15\ mg/m^3$.. In between the results of the two algorithms are interpolated to give the OC5CI value.

During the operational mission the ESA Near Real Time Level 1 data were used in order to provide the data in a timely manner for the numerical model. At the end of the mission delayed mode Non Time Critical data were used to provide improved accuracy. For the delayed data, Level 1 product is mapped to a gridded product at $300m$ resolution, with a single composite containing all the passes over the area of interest for each day.

The Sea and Land Surface Temperature Radiometer (SLSTR) carried onboard the Copernicus Sentinel 3A and Sentinel 3B satellites was used to calculate Sea Surface Temperature. Data were processed from EUMETSAT Level 2 data (Processing Baseline 3.7) by NEODAAS to create a single dataset for each day at 1 km resolution, taking the median over day and night passes. These data were used to provide additional context during the glider deployment, but were not assimilated by the numerical forecast model ~~.~~ which instead assimilated SLSTR SST observations processed by GHRSST (see Sec. 2.2.3).

Satellite data processing was carried out by the Natural Environment Research Council (NERC) Earth Observation Data Analysis and AI Service (NEODAAS).

2.2.3 Other Data Sources

In addition to the profiles from mission gliders and surface ocean colour from satellite, the physics observations assimilated were the same as in the Met Office's operational AMM15 forecasting system ~~(Tonani et al. (2019))~~(Tonani et al., 2019). These were satellite SST observations from various sensors downloaded from the Group for High Resolution Sea Surface Temperature (GHRSST), satellite sea level anomaly from various sensors downloaded from the Copernicus Marine Service, and in situ SST and temperature and salinity profiles downloaded from the Copernicus Marine Service and the Global Telecommunication System (GTS). These were processed, quality controlled and bias corrected as described by ~~Tonani et al. (2019)~~ Tonani et al. (2019).

2.3 Numerical Forecast Model

A physical-biogeochemical model, NEMO-FABM-ERSEM, with assimilation of observational data, was used to produce daily forecasts of the physical and biogeochemical state of the NWES. The set-up was based on the NWES configurations of the Forecasting Ocean Assimilation Model (FOAM) used for daily marine forecasting at the Met Office (FOAM-NWSO and FOAM-NWSBGC).

The physical component is based on version 3.6 of the Nucleus for European Modelling of the Ocean (NEMO, Madec and the NEMO team (2016)), specifically the AMM15 CO8 configuration ~~Graham et al. (2018); Tonani et al. (2019)~~ (Graham et al., 2018; Tonani e which covers the NWES at a horizontal resolution of 1.5 km. The vertical grid has 51 levels on a hybrid z-sigma terrain-following coordinate system ~~Siddorn and Furner (2013)~~(Siddorn and Furner, 2013). Atmospheric conditions at the surface were derived from the European Centre for Medium Range Weather Forecasting Integrated Forecasting System using CORE bulk formulae, as described by ~~Tonani et al. (2019)~~Tonani et al. (2019). The lateral boundary conditions for physical variables at the Atlantic boundary were taken from a Met Office global operational model and at the Baltic boundary from the Baltic Sea Analysis and Forecast product from the Copernicus Marine Service. In a later part of the investigation, the run was repeated using the AMM7 CO6 configuration ~~O'Dea et al. (2017); McEwan et al. (2021)~~(O'Dea et al., 2017; McEwan et al., 2021), which has a lower horizontal resolution, 7 km, but the same vertical grid. Lateral boundary conditions used the same sources as for AMM15, but surface forcing was derived from the Met Office global coupled numerical weather prediction system, as described by ~~Tonani et al. (2019)~~Tonani et al. (2019). Both AMM15 and AMM7 are run operationally at the Met Office, but only AMM7 is routinely run with a coupled biogeochemical model. This is the first demonstration of AMM15 with assimilation of biogeochemical observations.

The biogeochemical component of the forecasting model was the European Regional Seas Ecosystem Model (ERSEM, Butenschön et al. (2016))~~. ERSEM~~, which operates on the same numerical grid as NEMO. NEMO is one-way coupled to ERSEM using the Framework for Aquatic Biogeochemical Models (FABM, Bruggeman and Bolding (2014)), with ERSEM run at each NEMO timestep in each grid cell. ERSEM is a lower trophic level ecosystem model that includes pelagic plankton and benthic fauna ~~(Blackford (1997))~~(Blackford, 1997). ERSEM splits phytoplankton into four functional types largely based on their size ~~(Baretta et al. (1995))~~(Baretta et al., 1995): picophytoplankton, nanophytoplankton, diatoms and dinoflagellates. ERSEM uses variable stoichiometry for the simulated plankton groups and the biomass of each phytoplankton functional type (PFT) is represented in terms of chlorophyll, carbon, nitrogen and phosphorus, with diatoms also represented by silicon. ERSEM predators are composed of three zooplankton types (mesozooplankton, microzooplankton and heterotrophic nanoflagellates), with organic material being decomposed by one functional type of heterotrophic bacteria. The ERSEM inorganic component consists of nutrients (nitrate, phosphate, silicate, ammonium and carbon) and dissolved oxygen. The carbonate system is also included in the model, with total alkalinity and dissolved inorganic carbon as state variables.

~~NEMO is one-way coupled to ERSEM using the Framework for Aquatic Biogeochemical Models (FABM, Bruggeman and Bolding (201~~
~~), with ERSEM run at each NEMO timestep in each grid cell.~~

~~Observations are~~ Observations were assimilated daily using a 3DVar configuration of the NEMOVAR assimilation scheme ~~Mogensen et al. (2009); Waters et al. (2015); King et al. (2018). This uses~~ (Mogensen et al., 2009; Waters et al., 2015; King et al., 2018). This used a first guess at appropriate time method to assess model-observation differences, with model values interpolated to observation locations at the nearest model time step to the time of observation. ~~Glider~~ Similar to the existing operational approach for ocean colour Ford et al. (2012), the median value for glider measurements of chlorophyll, oxygen, temperature and salinity ~~were available every 6 hours, using the median value~~ in each model grid cell ~~for that~~ are taken every 6 ~~hour period in the assimilation~~hours. Daytime chlorophyll values ~~are~~ were not used, to avoid problems with fluorescence quenching. Background and observation error standard deviations for chlorophyll were the same as those used in the AMM7 operational system ~~Skákala et al. (2018)~~(Skákala et al., 2018), interpolated to the AMM15 grid. For oxygen a constant background to observation error ratio of 3 to 1 ~~is~~ was used. Temperature and salinity from the mission gliders are assimilated alongside profiles available in other parts of the domain using the same scheme as the operational AMM15 model ~~Tonani et al. (2019)~~ (Tonani et al., 2019). The correlation length scale used for chlorophyll and oxygen is the same as that for temperature in the operational AMM15 model ~~King et al. (2018)~~(King et al., 2018). Satellite values of chlorophyll concentration were provided as a combination of multiple passes for each day, so are taken to be valid at 12:00 UTC, the approximate time of satellite overpass. Increments for all variables are calculated using NEMOVAR and applied to the model using incremental analysis updates. For more information on the data assimilation see ~~King et al. (2018); Tonani et al. (2019); Skákala et al. (2021)~~ King et al. (2018); Tonani et al. (2019); Skákala et al. (2021).

2.4 Probabilistic Forecasting & Path Planning

The AI-driven path planning comprises two components: (a) a novel short-term stochastic forecast model which takes the deterministic numerical forecast to derive a probabilistic forecast of Chl-a and dissolved O2 within the operational region, and (b) a path planning concept which utilises the probabilistic forecast information to yield the most useful paths fit for the science and operational purpose for the multiple gliders.

The short-term probabilistic forecast is based on Bayesian methods, which offer several advantages including incorporation of prior knowledge, intuitive uncertainty quantification, and effective modeling of spatial and temporal dependencies (Blangiardo et al., 2013; Lindgren and Rue, 2015; Salim et al., 2025; Palmí-Perales et al., 2025; Wang et al., 2025; Skakala et al., 2023). Specifically, we use the Integrated Nested Laplace Approximation (INLA) method ~~(Blangiardo et al. (2013))~~(Blangiardo et al., 2013), combined with the Stochastic Partial Differential Equation (SPDE, ~~Lindgren et al. (2011)~~Lindgren et al. (2011)). This approach is a computationally efficient method for both spatial and spatio-temporal models ~~(Rue et al. (2009); Lindgren and Rue (20~~ ~~)~~(Rue et al., 2009; Lindgren and Rue, 2015).

The probabilistic model takes input from the deterministic numerical model. Each day, it uses the most recent historical data (last five days) plus a short-term forecast (three days, including the current day) to predict the uncertainty associated with conditions ~~on days 6 and 7~~ in the forecast period for the key target variables chlorophyll-a and dissolved oxygen. This provides mean estimates as well as covariance information (upper and lower limits of uncertainty bound) over the required spatio-temporal domain. These uncertainty estimates are critical because they enable the path planner to go beyond simply targeting predicted ~~maxima or~~ chl-a maxima or oxygen minima; instead, it can strategically direct the gliders to areas where the model's confidence is lowest. This approach allows the gliders to collect data that most effectively reduces prediction uncertainty and improves the overall performance and reliability of the numerical model.

From this, navigational waypoints are determined regularly for the three gliders to cover a distance of $20km$ over 24-hour periods. Initially, the path planning strategy focused on reducing model uncertainty by prioritising navigation of gliders toward locations with the greatest difference between the upper and lower uncertainty bounds, i.e., the largest levels of uncertainty in the prediction or forecast variance. However, since the largest uncertainty was consistently observed near the operational boundaries, which are less informative for operational sampling, the strategy was revised. The approach shifted to transect-based sampling of the feature of interest, focusing on the predicted mean state gradients, disregarding forecast uncertainty in

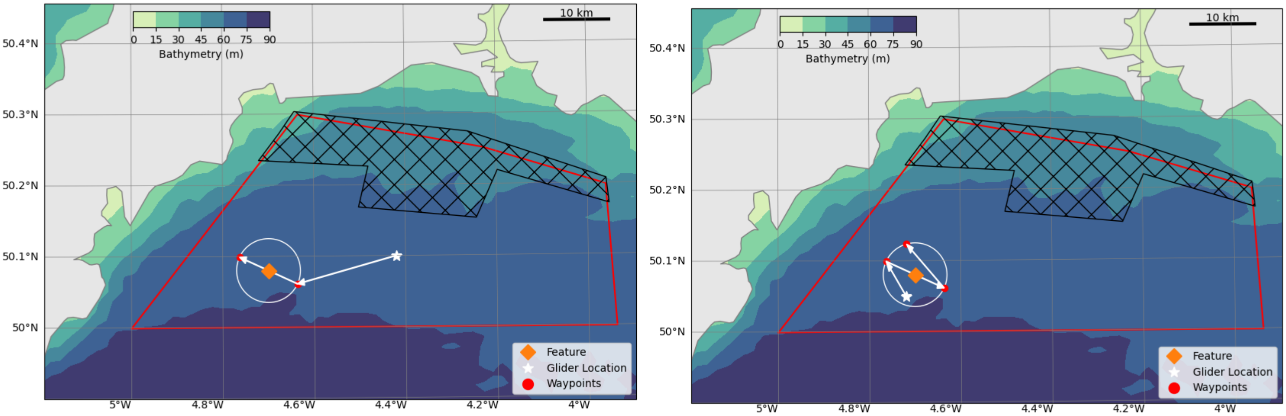

Figure 2. Path planning scenarios for a feature of interest (diamond). A $5km$ radius circle drawn around the feature, if the glider is currently outside the circle waypoints are set to navigate to the circle boundary and transect across (left). If inside, systematically cover the circled region (right). Hatched areas are too shallow to safely operate the gliders, dashed red line used as a boundary for path planning

the path planning decisions. This revised strategy is shown in Fig. 2.

The boundary of the glider operational region is marked in Fig. 2 with a solid red line, with the hatched region at the northern part of the operational region the typical no-go shallow zone for the class of gliders. To account for tidal advection pushing the gliders off course, a broad 5km buffer zone is also applied around the edges for safety, as indicated by dashed red line.

From the probabilistic model, the location of a feature of interest is identified in the forecast period (e.g. maximum chlorophyll-a, minimum dissolved oxygen or maximum uncertainty). A $5km$ radius circle is created with the location as its center. The intention here is that the glider performs a transect along the direction of the dominant gradient of the feature within the identified circle.

If the initial location of the glider is outside the feature circle, the waypoints for the glider transect path are determined as follows: First, the dominant gradient path across the circle through the feature is calculated. Then the locations were this path crosses the circle are identified, with the closest point to the gliders current location used as the first waypoint. Lastly, the waypoints are set so that the glider proceeds along the dominant gradient path across the circle, as shown in the left subplot of Fig. 2.

Conversely, if the initial location of the glider is already inside the feature circle, waypoints are instead set to transect back and forth within the circle along the dominant gradient. When the glider path reaches the circumference of the circle, the dominant gradient is reversed and and offset by a small angle to maximize are coverage, as depicted in the right subplot of Fig. 2.

2.5 Daily cycling during the field campaign

The operational window for the glider mission occurred in Aug-Sep 2024. During the operational glider deployment, the forecasting model was run daily at 08:30 UTC. An analysis step with data assimilation was run for the previous day, following which the model ran forwards without assimilation for 3 days to provide a forecast for 2 days ahead. Model outputs were post-processed to give values at fixed depths (z-levels) for chlorophyll and dissolved oxygen in the region around the glider deployment area (dashed line in 1), which were then passed to the probabilistic and path planning models by 13:00 UTC. The path-planning model produced waypoints by 16:00 for each glider for the following 24-48 hours. These waypoints underwent human pilot checks for approval to ensure maritime safety before being transmitted via iridium satellite to the gliders while they were held at the sea surface. Glider data and satellite data were collected and provided to the model the following day and the cycle repeated.

2.6 Mission Summary

The mission provided numerous operational challenges. For the gliders this included occasional technical and communication failures, as well as some more critical vehicle and sensor issues which prompted a number of recovery and redeployment cycles. Unit 482 suffered a critical fault after two weeks and was not redeployed after recovery on 21st August 2024. Units 480 and 481 continued to operate until 30 August 2024, after which the campaign relied solely on Unit 480. This glider was recovered on 14 September for recharging and maintenance and was redeployed on 18 September alongside unit 481, both of which remained operational until the end of the observational campaign on 28 September 2024.

The operational area, shown by the red bounding box in Fig 1 and 2, posed additional challenges. Shallow ~~diving depths and occasionally~~ depths limited the available region and strong currents resulted in gliders occasionally moving outside the designated area. This was mitigated in part by ~~occasional~~ the use of onboard thrusters controlled by remote human operators.

In total, glider observations were successfully obtained on 49 out of 54 days (6th August - 28th September 2024), providing 90% mission coverage. Of these, 15 days (28%) included all three gliders operating simultaneously, 21 days (39%) involved two gliders, and 13 days (24%) had a single glider in operation. Only 5 days (9%) were without glider activity.

The numerical simulations also featured many challenges. Communication failures occasionally meant simulations ran without the latest observational data. Additionally the simulations were performed on research infrastructure where the availability of computational resources was a limiting factor resulting in a delay producing the forecast data.

Development of the probabilistic forecast and path planning system meant the system was not active at the start of the mission, first entering operation on the 16th August. Delays in receiving the forecast data or other computational issues resulted in some days when no new waypoints were generated. In that scenario the gliders were instructed to repeat the previous day's waypoints to maintain continuous operation. We implemented the first path planning strategy, focused on uncertainty reduction, from 16th August to 7th September, and then switched to the second, transect-based approach from 9th September until 24th September.

During the mission period a Karenia bloom was observed via satellite in the Celtic Sea, but it did not migrate into the English channel (Shutler et al., 2012). The glider network therefore had no opportunity to navigate to and measure the bloom over the operational period.

Despite these challenges, there were several periods where the entire DTO system was fully operational without human intervention, outside of standard monitoring and quality assurance.

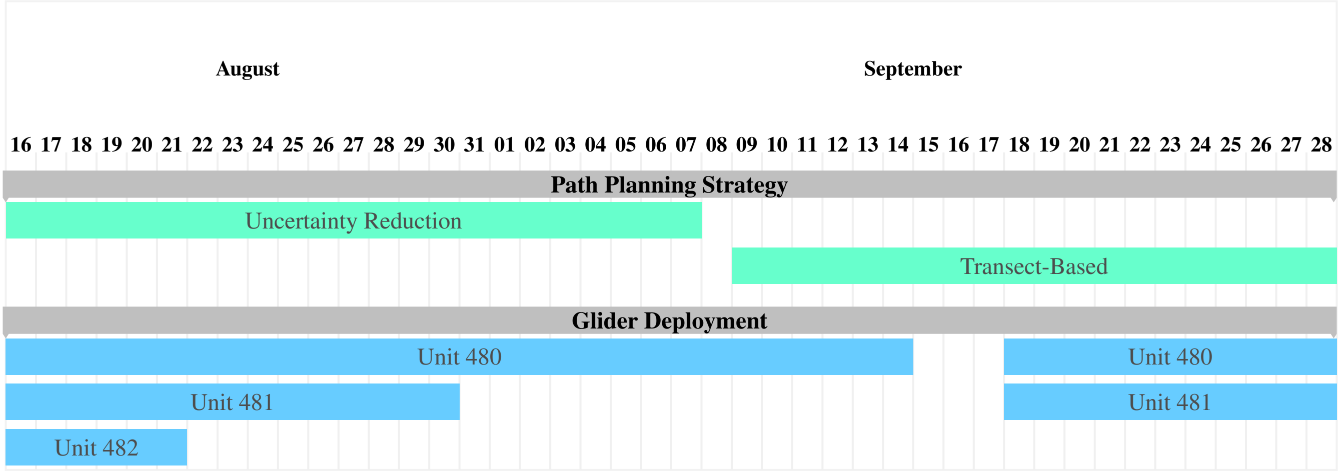

Figure 3. Mission Summary of glider deployment and path planning strategies used

3 Post-Mission Analysis

~~The scope of this manuscript is primarily on the numerical modelling components and outcomes of the digital twin architecture, focusing~~ After the mission, a review of the various components of the DTO was carried out, with a series of additional simulations performed to focus on the impact that multiple co-ordinated gliders can have on the ability of the system to forecast observed conditions, or what might be considered the accuracy of the *virtual twin*. Assessment includes consideration of how increased resolution in the numerical model captures natural variability and features that are less well resolved in lower resolution, along with estimates for how the path planning component differs when the glider observations are not assimilated.

3.1 Experiments

As part of the post-mission analysis a series of experiments have been designed to explore the impact of observation processing and model resolution on the performance of the DTO. In total 4 simulations have been performed and will be reviewed in this paper:

- AMM15-NRT - Experiment ~~assimilating NRT~~ on the 1.5km grid assimilating near real time (NRT) SST and Chlorophyll-a, along with NRT glider profiles of Temperature, Salinity, Chlorophyll-a and Oxygen. This run is identical to the one that ran operationally during the mission, with none of the issues that occurred in real-time.
- AMM15-NoG - Experiment assimilating NRT SST and Chlorophyll-a observations, akin to the current operational system but without assimilation of glider data.
- AMM15-DT - Experiment assimilating the ~~datasets from~~ same observational datasets as AMM15-NRT~~after they have gone through~~ , with Chlorophyll-a satellite data and glider profiles undergoing additional post-processing (aka delayed time (DT) observations).
- AMM7-NRT - Experiment using the same observations as AMM15-NRT on the lower resolution AMM7 domain.

3.2 Impact of Gliders

~~Taking~~ Ford et al. (2022) demonstrated that assimilating glider observations can have a large impact on model forecasts of chlorophyll. Fig. 4 shows the correlation between model and observation for the AMM15-NoG and AMM15-NRT experiments. Here the improvement from assimilating glider chlorophyll measurements results in a 32% reduction in RMSE and an improvement in the correlation. For O_2 the improvements are even greater, with a 57% reduction in RMSE. This is due to the gliders representing the only source of oxygen measurements assimilated in the system.

By assuming delayed time observations are the optimal observations and data assimilation improves model predictions, we can assume AMM15-DT (as defined in Sec.3.1) ~~as~~ is the best possible representation of the ocean state ~~, the other runs can be evaluated against it~~available. Figure 5 shows the root mean square deviation (RMSD) for the other two AMM15 simulations [AMM15-NoG and AMM15-NRT] against the delayed time run for chlorophyll-a. At the surface, the RMSD shows similar differences between the simulation using NRT data and the run with no gliders. This is likely due to the surface in the simulation being primarily impacted by satellite data, the assimilation of which was identical in both AMM15-NRT and AMM15-NoG. However, the impact of the gliders is shown to be significantly higher in ~~the depth averaged results~~ results averaged over the entire water column, with large differences evident where no glider data has been assimilated. Despite a relatively small operating area (red box), the glider impact covers a large distance, particularly to the south west of the zone. For the NRT run, the difference is comparable to the surface RMSD, indicating that the impact of using delayed time gliders over near real time is smaller than the impact of using delayed time satellite data over near real time satellite data.

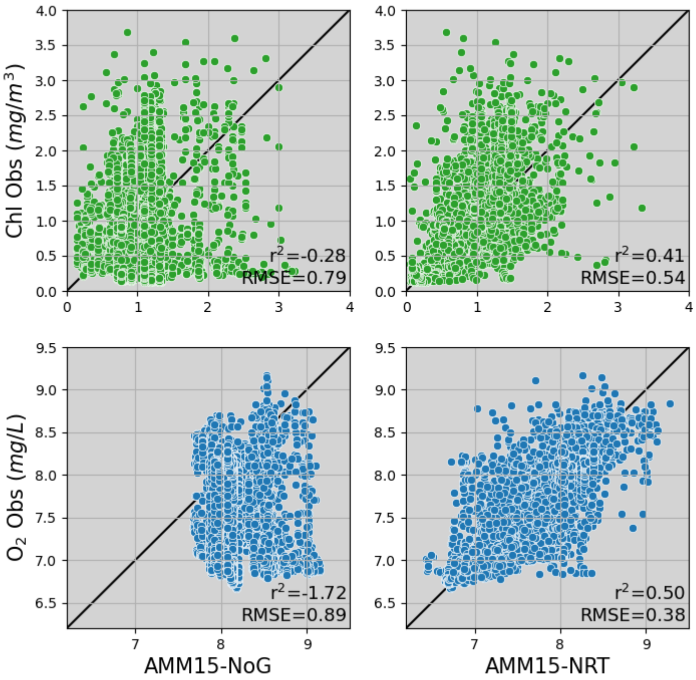

Figure 4. Glider observations of Chlorophyll-a (top) and Oxygen (bottom) versus model predictions with no glider assimilation (left) and with (right).

A large element of the digital twin is the ability to produce informative forecasts to guide the path planning element. Figure 6 shows the RMSD of the day 1, 2 and 3 forecasts against the AMM15-DT analysis solution. For temperature, after a week from when the gliders start collecting data the difference without gliders at 1-day lead time is greater than near real time gliders at 2-days and similar to NRT 3-days ahead. For chlorophyll there is minimal difference between the two simulations, which suggests that averaged over a spatial region the size of the difference between processing levels is of a similar scale to the difference between including and excluding gliders. At 3-day lead time the difference to the analysis is around double that of the 1-day lead time, implying that without continual assimilation the model will drift away from the true state.

As part of the mission plan the gliders are targeting so-called ’event states’, thresholds which indicate a feature of interest has developed. The thresholds are defined to be greater than $2.5mg/m^3$ for chlorophyll (a typical bloom indication level), and below $6mg/L$ for oxygen (based upon OSPAR thresholds for the north west European shelf). Figure 7 shows the number of days the threshold is reached over the mission period between simulations with and without glider assimilation. For Chlorophyll-a the event state is triggered significantly more to the south west of the domain, consistent with the changes shown

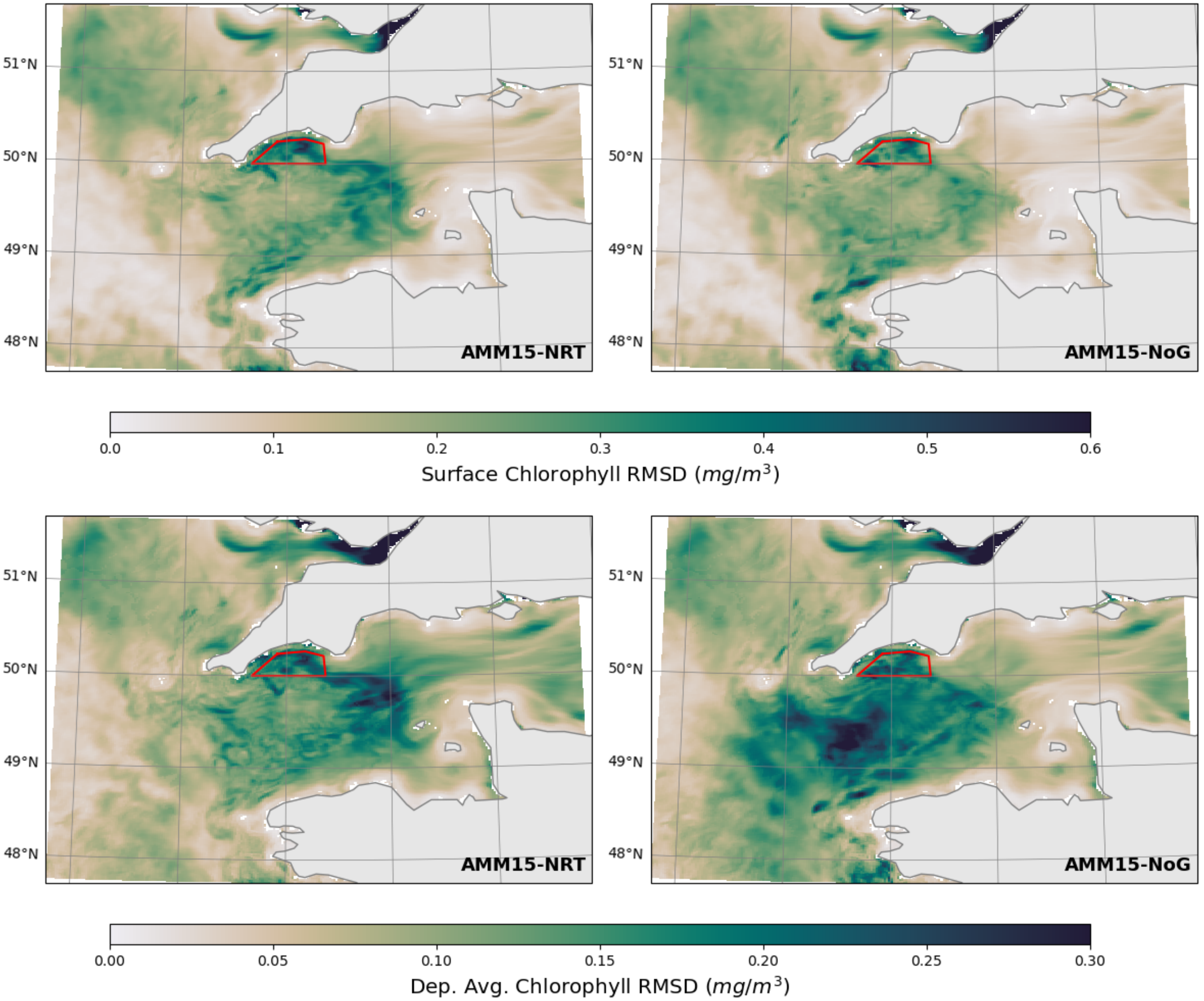

Figure 5. Time-averaged RMSD of the analysis fields for AMM15-NRT (left) and AMM15-NoG (right) against the AMM15-DT simulation across the simulation period for surface only (top) and ~~depth~~ water column averaged (bottom) fields. The glider operating area is indicated by the red box.

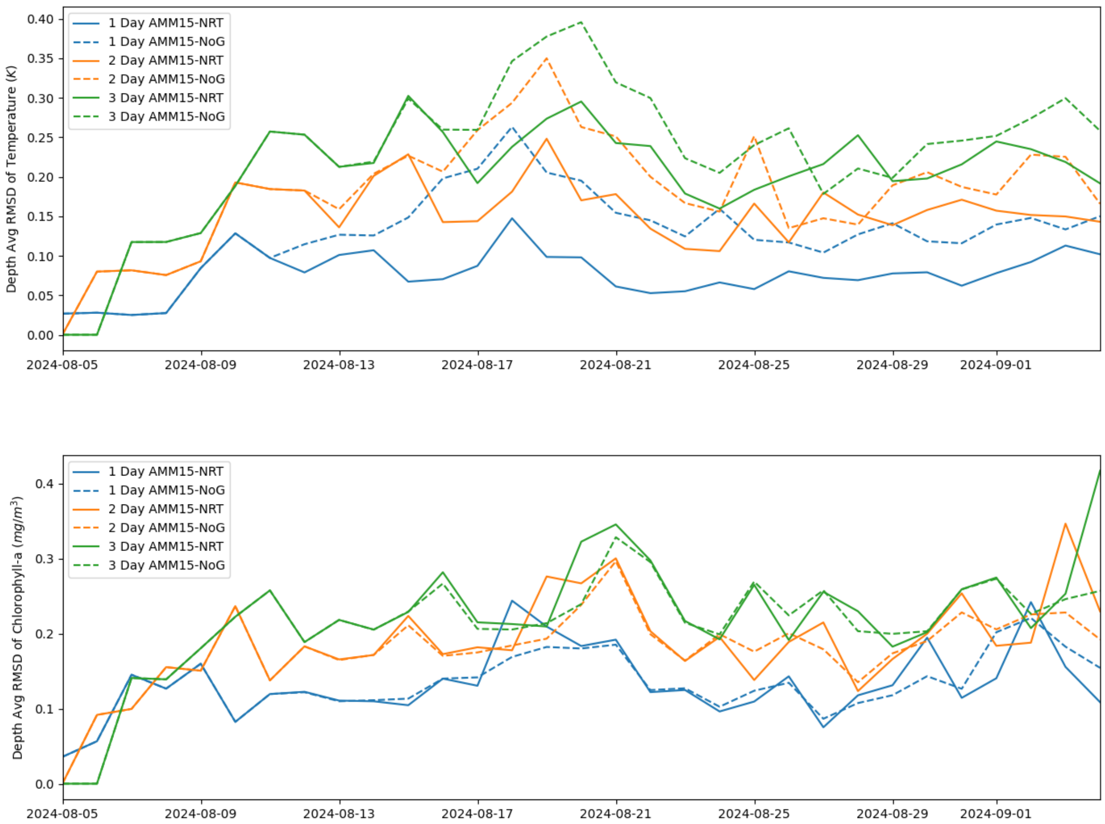

Figure 6. Spatially-averaged RMSD of forecasts from AMM15-NRT (solid lines) and AMM15-NoG (dashed lines) against the AMM15-DT analysis at different forecast lengths. Top - ~~depth averaged~~ average water column temperature, bottom - ~~depth averaged~~ average water column chlorophyll-a.

with the assimilation previously. Inside the operational zone the event state would trigger on 2-3 extra occasions when glider data is assimilated. With dissolved oxygen, there is a notable increase in hypoxic events in the English Channel that were not identifiable without gliders, although within the operational zone there were no events.

3.3 Impact of Resolution

Comparison of the AMM15-NRT 15km and AMM7-NRT 7km resolution models reveal that there is a truly substantial impact of model spatial resolution (and the associated changes) on the inputs for the glider path planning. Whilst the two resolution models are not like-for-like prohibiting a full direct comparison, the two resolution models show large differences in the two essential biogeochemistry variables provided for the glider, chlorophyll-a and dissolved oxygen (Fig.8). ~~In case~~ Some of this can be attributed to a difference in initial conditions, particularly for bottom dissolved oxygen where the differences are

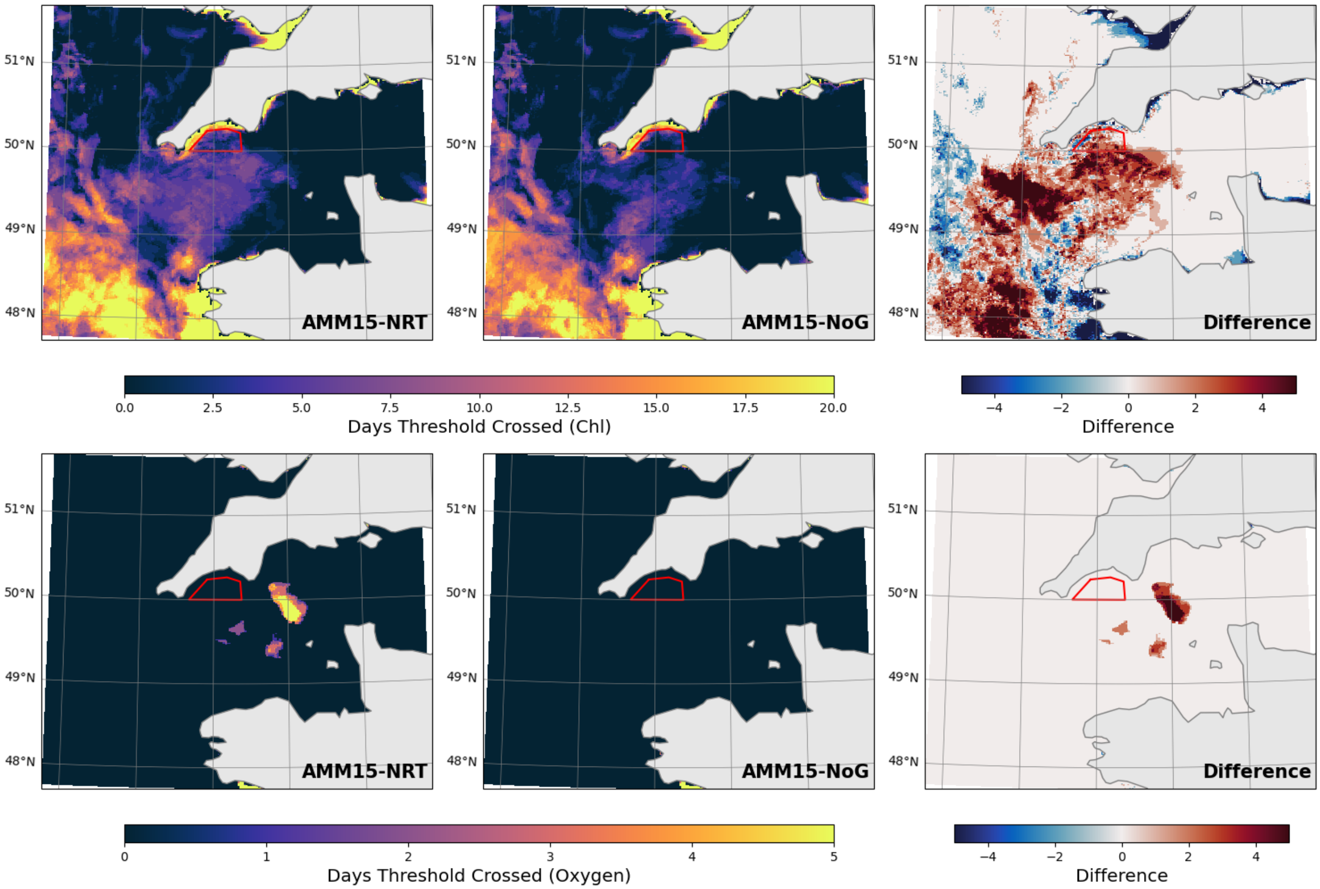

Figure 7. Instances the event state threshold is crossed anywhere in the water column for chlorophyll-a (top) and oxygen (bottom) for the AMM15-NRT (left), AMM15-NoG (middle) and the difference between them (right)

consistently large across the domain and the forecast lead time. In this case the glider oxygen assimilation is seen to have limited impact in bringing the different resolution models closer together. In case of surface chlorophyll-a, the model differences are substantially reduced in the analysis by the assimilation of the abundant satellite data, as well as the gliders, but those differences quickly grow in the model forecast ~~. For bottom dissolved oxygen, the differences are consistently large across the domain and the forecast lead time, so the glider oxygen assimilation is seen to have limited impact in bringing the different resolutionmodels closer together~~highlighting the significance of grid resolution.

The differences shown in Fig.8 arise due to dynamical impact of the higher (1.5km) spatial resolution on the biogeochemistry, as perceived on the 7km scale. There is however additional benefit of the 1.5km resolution model that comes from providing outputs at the finer 1.5km spatial scale. This is assessed by Fig.9 showing the 1.5km spatial scale variability of chlorophyll-a and dissolved oxygen that is unresolved at the 7km scale. This variability is considerable especially for chlorophyll, but is smaller than the differences between the two resolution models at 7km scale. For example the 1.5km model at its resolution scale has a wider range of dissolved oxygen values, (4.5-13 mg/L), compared to the 7km model (6.2-9 mg/L). However even after upscaling the 1.5km model oxygen outputs to the 7km scale, the interval of oxygen values remains almost as wide as on the 1.5km scale (5.12-12.5 mg/L), and much wider than in the 7km resolution model. In each case the 1.5km model includes cases of moderate hypoxia (4-6mg/L), whilst the 7km model did not see hypoxia at all. Not surprisingly, the 7 km scale differences between the two resolution models, as well as the unresolved variability of the 1.5km resolution model, are the greatest in the coastal areas (Fig.8-Fig.9), where fine spatial resolution matters most.

The impact of the model differences on the glider path planning can be understood from Fig.10 and Fig.11. Unlike the 1.5km model where the threshold for high chlorophyll-a values is met on a big part of the domain including the glider area, in the 7km model it is crossed only in very limited locations at the analysis time and in the next day's forecast. When it comes to dissolved oxygen, hypoxic events could be seen on a range of days in the coastal areas and western English Channel (including within the glider opration area) in the 1.5km model, but the hypoxia threshold of 6mg/L was never crossed within the 7km resolution model.

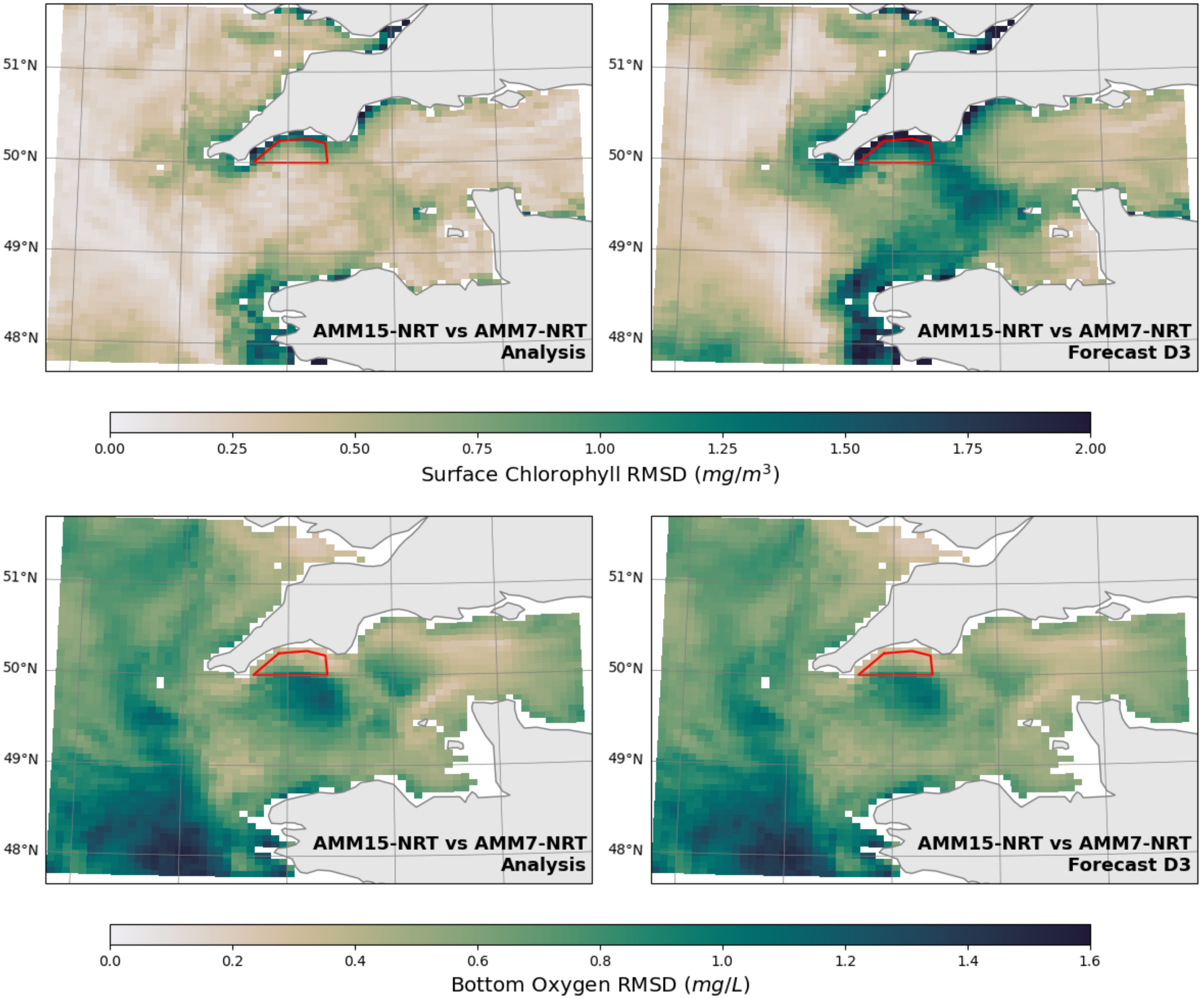

Figure 8. Time-averaged RMSD of the 1.5km resolution and 7km resolution model total surface chlorophyll-a in mg/m^3 (top) and bottom dissolved oxygen in $mmol/m^3$ (bottom) for the analysis (left) and at 3-day lead time (right). As in the previous Figure, the 1.5km model has been upscaled to the 7km model grid.

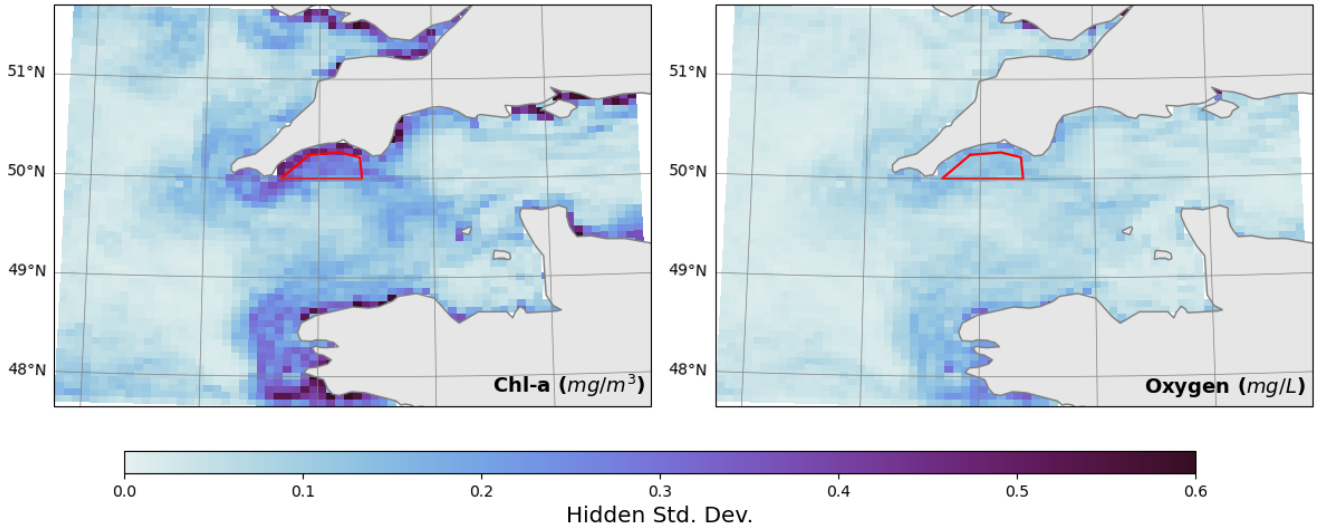

Figure 9. Variability represented by the 1.5km resolution model, but hidden (averaged out) on the 7km resolution model scale. The plots show the time-averaged third forecast day standard deviation for chlorophyll-a (in mg/m^3, left-hand panel) and bottom dissolved oxygen (in mg/L, right-hand panel).

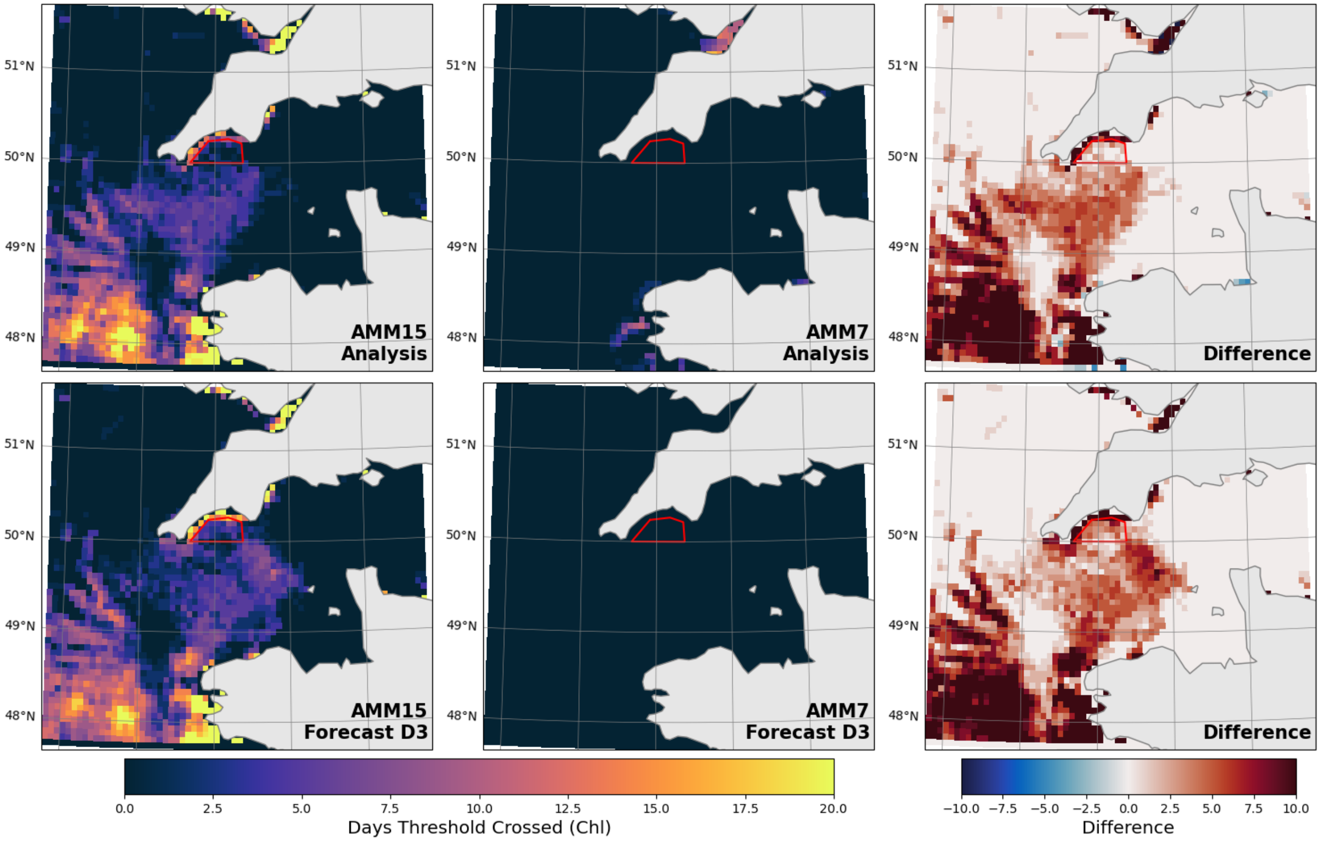

Figure 10. Number of mission days on which chlorophyll-a concentration crossed the 2.5 mg/m^3 threshold (anywhere in the water-column) on the 7km spatial scale in the two models: (i) the 1.5km resolution model in the left-hand panel, and the (ii) 7km resolution model in the right-hand panel. The 1.5km resolution model data have been upscaled to the 7 km model grid before the number of days was calculated.

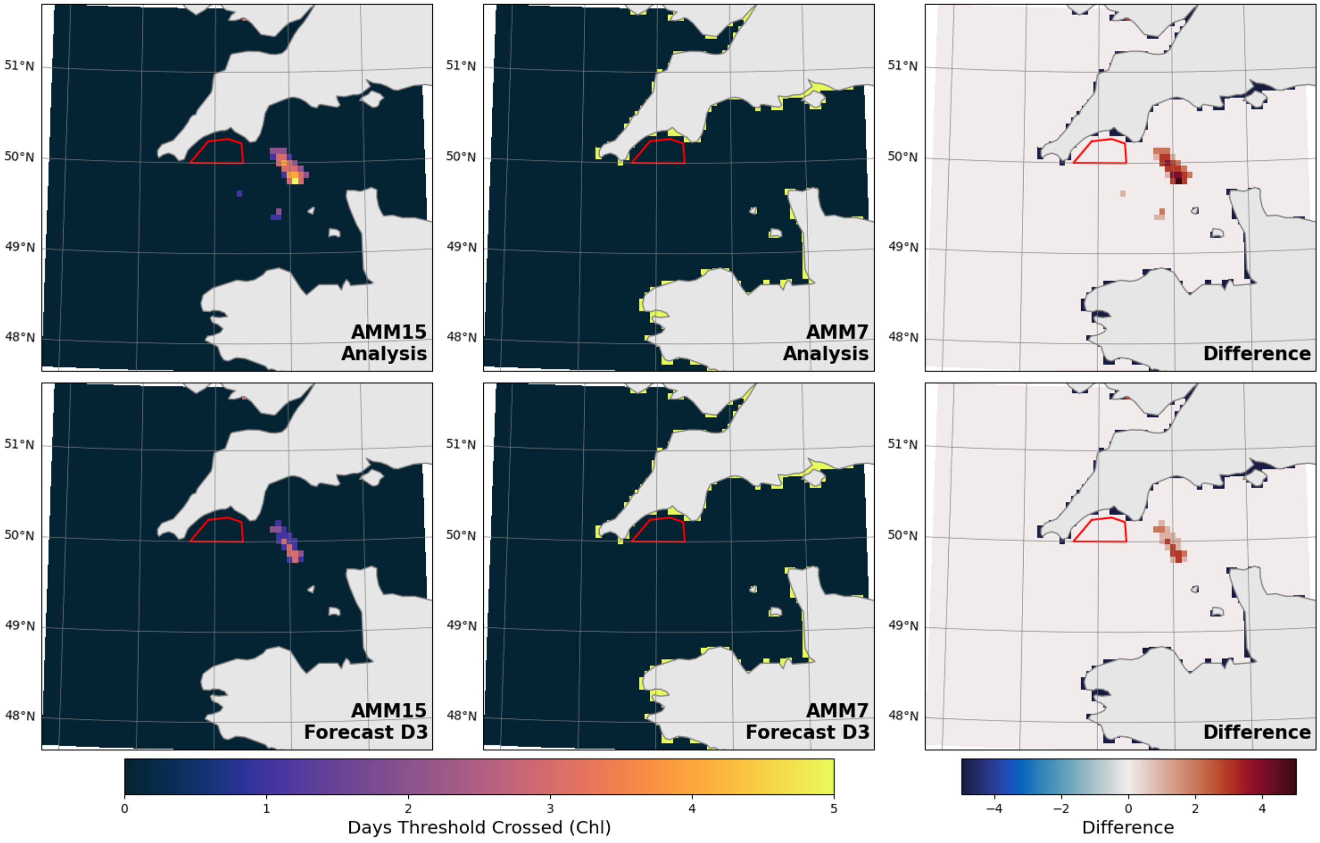

Figure 11. Number of mission days on which dissolved oxygen concentration crossed the 6 mg/L threshold (anywhere in the water-column) on 7km spatial scale in the two models: (i) the 1.5km resolution model in the left-hand panel, and (ii) the 7km resolution model in the right-hand panel. The 1.5km resolution model data have been upscaled to the 7 km model grid before the number of days was calculated.

3.4 Impact of Gliders on Path Planning

As part of the post-mission reanalyses the probabilistic forecast and path planning has been run using outputs from both AMM15-NRT and AMM15-NoG for comparison. The run sets paths for two gliders, with one targeting maximum chlorophyll and the other minimum oxygen. As this is being performed post-mission the paths will be decoupled from the actual gliders that provided measurements for the assimilation.

The post-mission paths are shown in 12. The paths set for the glider targeting chlorophyll go back and forth across the area regardless of the dataset being used, suggesting either high uncertainty with regards to the maximum chlorophyll location, or multiple local maxima in the area. On the other hand, the glider targeting minimum oxygen stayed within a more contained area, albeit with an offset in the location between the two model simulations. As oxygen dynamics are slow moving compared to chlorophyll, this suggests that without glider assimilation the equipment would not be in the optimal location to gather information.

To get a scale of how sub-optimal the location is we can consider the distance between the waypoints for each glider path, shown in 12. Here the distance for the chlorophyll targeting glider oscillates, reflecting the paths crossing back and forth. However the oxygen targeting glider increases throughout the mission time up to around $20km$, meaning if the minimum zone is a localised event the glider would be almost a full day of travel away.

4 Conclusion

This paper has presented an exciting ~~new~~ Digital Twin Ocean framework that enables a continual two-way coupling between real and virtual environmental systems via a continuous feedback loop of measure, predict, direct and refine. Building on a pilot study of ~~Ford et al. (2022)~~(Ford et al., 2022), every element of the digital twin has evolved to optimise the overall impact of the system.

We show that the inclusion of multiple in-situ glider observations within higher resolution models significantly improves the data assimilation product and subsequently the predictive skill of the model. This extends beyond immediate reduction of bias/error at the time of assimilation to recognisable improvement over the short-term forecast period. Instances where the forecast predicts ~~key thresholds to be crossed also increase~~ the crossing of key thresholds in both chlorophyll and dissolved oxygen also increase with the inclusion of these glider measurements, ~~highlighting the potential to capture~~ resulting in a system that captures extremes more readily and accurately.

The numerical model used in this study also benefits from increased resolution compared to previous work ~~Ford et al. (2022)~~ (Ford et al., 2022), capturing features that would have previously been missed at the current UK operational resolution~~, in which~~ . In the current operational system much of the natural variability in the system is lost, especially close to the coast.

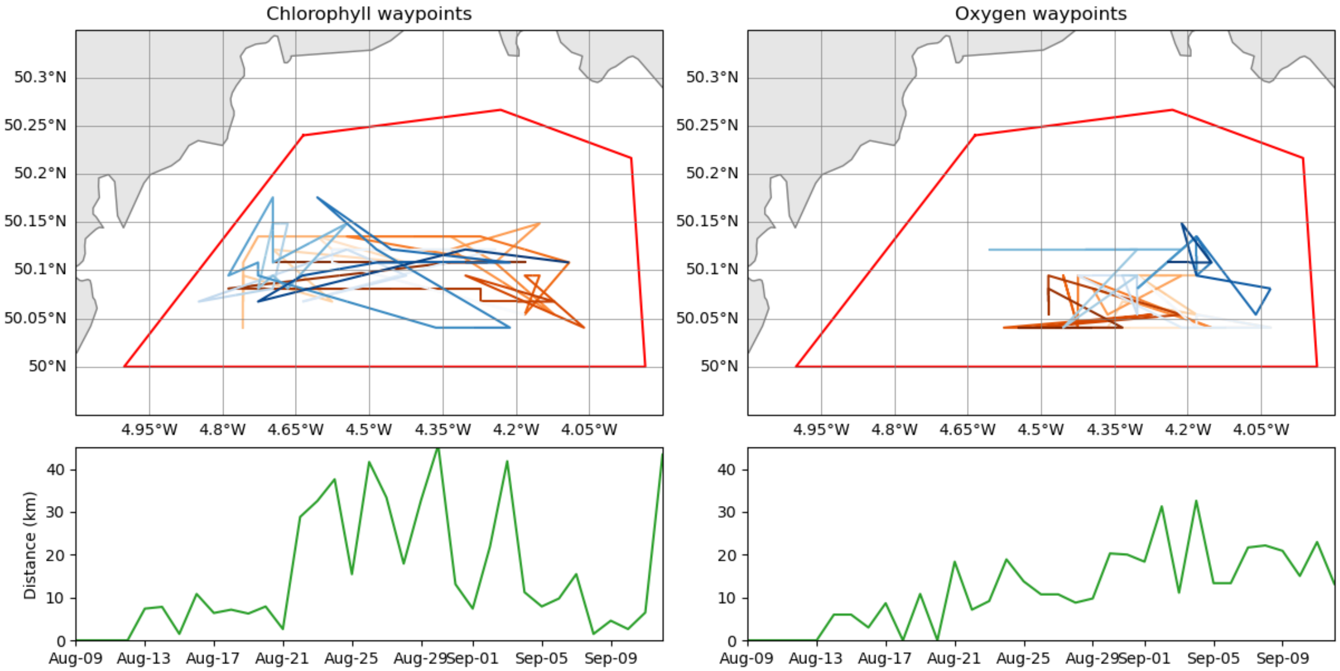

Figure 12. Top - Paths for two gliders set using AMM15-NRT (Blue) and AMM15-NoG (Orange), with darkness of line indicating time. Left - glider targeting maximum chlorophyll, Right - glider targeting minimum oxygen. Bottom - Hypothetical distance between glider waypoints

Additionally, several instances of the key threshold for chlorophyll are identified ~~,~~ that were otherwise missed, whilst some dissolved oxygen events are predicted that are missed entirely at the lower resolution.

The two-way coupling and path planning algorithm provided valuable improvements to navigation of the gliders, ~~with the potential to otherwise produce errors of up to tens of kilometers, significantly increasing the chance of~~ locating and better resolving target events as ~~the evolve.~~

they evolve. Using multiple gliders has also proven to be a major asset, as the oxygen minima were largely misaligned with the chlorophyll maxima (or other key features), so they could not both be captured by the same single glider. ~~Furthermore using the data in the delayed mode had significant~~

Assimilating delayed mode data was also shown to alter the results from simulations with near real time observations, with an impact on glider navigation~~, so any~~. Any future mission could substantially benefit from speeding up the data processing in real time to make use of these observations.

The DTO system provides many exciting opportunities for the future, including: i) addressing challenges with combining in-situ measurements alongside satellite fields within data assimilation through cross-calibration and bias correction, ii) accounting for the multi-scale issues in estimating error covariance matrices and representativeness errors, making use of diagnostics such as ~~Fowler et al. (2023)~~(Fowler et al., 2023), iii) adding automatic imaging cameras to the gliders to better distinguish phytoplankton species and iv) using ML to speed up prediction and derive addition information, such as the likelihood a chlorophyll bloom is due to *Karenia mikimotoi*.

This work represents a major advance in our ability to deploy a true Digital Twin Ocean, that not only improves model outputs through the ingestion and assimilation of observational data, but that optimises both the predictive capability of the virtual twin, while improving the effectiveness of the real-world monitoring strategy. This framework has immediate value to those requiring near real-time understanding of complex environmental systems for improved management and early warning systems.

Code and Data Availability

All glider locations and profiles, surface satellite fields and numerical model output is available to visualise and request through the Synced-Ocean data portal (https://synced-ocean.eofrom.space/). Any additional data supporting this work can be made available upon request.
Details of how to download the physical ocean model NEMO-FABM can be found at https://doi.org/10.5281/zenodo.7732984, and the biogeochemical model ERSEM can be found at https://zenodo.org/badge/latestdoi/302390544. Due to intellectual property copyright restrictions the source code for NEMOVAR cannot be provided.

Author Contribution

DP, DF, SK and AR set up and ran the pseudo-operational forecasting system. DP ran the AMM15 post mission experiments, and DB ran the AMM7 experiment. KW and PM developed and ran the probabilistic forecast model and path planning algorithm. JW processed and quality controlled the glider data. DC and ES processed and quality controlled the satellite data. MP supervised the Synced-Ocean project. DP, JS and DB performed analysis of the post mission experiments. DP led the writing of the manuscript, with contributions to the writing and editing from all authors.

Competing Interests

The authors declare that they have no conflict of interest.

Acknowledgements

The authors thank the crew of the RV Plymouth Quest and RV Plymouth Sepia for their support at sea, and the NERC Earth Observation Data Analysis and Artificial-Intelligence Service (NEODAAS) for supplying data for this study.
This study has been conducted using E.U. Copernicus Marine Service Information: doi:10.48670/moi-00010

Financial Support

SyncED-Ocean was funded through the NERC-Met Office funded Twinning Capability for the Natural Environment (TWINE) programme, grant number NE/Z50337X/1.

References

Baretta, J., Ebenhöh, W., and Ruardij, P.: The European regional seas ecosystem model, a complex marine ecosystem model, Netherlands Journal of Sea Research, 33, 233–246, 1995.

Barnes, M. K., Tilstone, G. H., Smyth, T. J., Widdicombe, C. E., Gloël, J., Robinson, C., Kaiser, J., and Suggett, D. J.: Drivers and effects of Karenia mikimotoi blooms in the western English Channel, Progress in Oceanography, 137, 456–469, 2015.

Bittig, H. C., Fiedler, B., Scholz, R., Krahmann, G., and Körtzinger, A.: Time response of oxygen optodes on profiling platforms and its dependence on flow speed and temperature, Limnology and Oceanography: Methods, 12, 617–636, 2014.

Blackford, J.: An analysis of benthic biological dynamics in a North Sea ecosystem model, Journal of Sea Research, 38, 213–230, 1997.

Blangiardo, M., Cameletti, M., Baio, G., and Rue, H.: Spatial and spatio-temporal models with R-INLA, Spatial and spatio-temporal epidemiology, 4, 33–49, 2013.

Bruggeman, J. and Bolding, K.: A general framework for aquatic biogeochemical models, Environmental modelling & software, 61, 249–265, 2014.

Buck, J. J., Lopex, A. L., Hawes, N., Allsup, B., Dobra, T., Ferreira, T., Kokkinaki, A., Morris, A., Lacerda, B., Patmore, R., et al.: A Marine Autonomous Systems Digital Twin; Bringing value to researchers, data users and vehicle operations, in: OCEANS 2024-Halifax, pp. 1–4, IEEE, 2024.

Butenschön, M., Clark, J., Aldridge, J. N., Allen, J. I., Artioli, Y., Blackford, J., Bruggeman, J., Cazenave, P., Ciavatta, S., Kay, S., et al.: ERSEM 15.06: a generic model for marine biogeochemistry and the ecosystem dynamics of the lower trophic levels, Geoscientific Model Development, 9, 1293–1339, 2016.

Ford, D., Edwards, K., Lea, D., Barciela, R., Martin, M., and Demaria, J.: Assimilating GlobColour ocean colour data into a pre-operational physical-biogeochemical model, Ocean Science, 8, 751–771, 2012.

Ford, D. A., Grossberg, S., Rinaldi, G., Menon, P. P., Palmer, M. R., Skákala, J., Smyth, T., Williams, C. A., Lorenzo Lopez, A., and Ciavatta, S.: A solution for autonomous, adaptive monitoring of coastal ocean ecosystems: Integrating ocean robots and operational forecasts, Frontiers in Marine Science, 9, 1067 174, 2022.

Fowler, A. M., Skákala, J., and Ford, D.: Validating and improving the uncertainty assumptions for the assimilation of ocean-colour-derived chlorophyll a into a marine biogeochemistry model of the Northwest European Shelf Seas, Quarterly Journal of the Royal Meteorological Society, 149, 300–324, 2023.

Garau, B., Ruiz, S., Zhang, W. G., Pascual, A., Heslop, E., Kerfoot, J., and Tintoré, J.: Thermal Lag Correction on Slocum CTD Glider Data, Journal of Atmospheric and Oceanic Technology, 28, 1065 – 1071, https://doi.org/10.1175/JTECH-D-10-05030.1, 2011.

Graham, J. A., O'Dea, E., Holt, J., Polton, J., Hewitt, H. T., Furner, R., Guihou, K., Brereton, A., Arnold, A., Wakelin, S., et al.: AMM15: a new high-resolution NEMO configuration for operational simulation of the European north-west shelf, Geoscientific Model Development, 11, 681–696, 2018.

Halvorsen, D. Ø., Chiatante, C., Penne, C. L., Singh, A., Bakken, S., Fragoso, G. M., Birkeland, R., Dallolio, A., Garrett, J. L., Johansen, T. A., Ellingsen, I. H., and Alver, M. O.: Operational Closed-Loop System for Multi-Scale Chlorophyll-a Monitoring along the Norwegian Coast, Frontiers in Marine Science, 13, https://doi.org/10.3389/fmars.2026.1688255, 2026.

King, R. R., While, J., Martin, M. J., Lea, D. J., Lemieux-Dudon, B., Waters, J., and O'Dea, E.: Improving the initialisation of the Met Office operational shelf-seas model, Ocean Modelling, 130, 1–14, 2018.

Lee, J.-H., Nam, Y.-S., Kim, Y., Liu, Y., Lee, J., and Yang, H.: Real-time digital twin for ship operation in waves, Ocean Engineering, 266, 112 867, 2022.

Lindgren, F. and Rue, H.: Bayesian spatial modelling with R-INLA, Journal of statistical software, 63, 1–25, 2015.

Lindgren, F., Rue, H., and Lindström, J.: An explicit link between Gaussian fields and Gaussian Markov random fields: the stochastic partial differential equation approach, Journal of the Royal Statistical Society Series B: Statistical Methodology, 73, 423–498, 2011.

Madec, G. and the NEMO team: NEMO ocean engine, v3.6, Institut Pierre-Simon Laplace, France, https://doi.org/10.5281/zenodo.1472492, 2016.

Mansfield, T., Wihsgott, J., Skakala, J., Menon, P., Gardner, E., Kay, S., and Palmer, M.: Lessons learned in establishing an environmental digital twin, Oceans 2025 Proceedings, in press, 2025.

McEwan, R., Kay, S., and Ford, D.: Quality Information Document for the CMEMS North West European Shelf Biogeochemical Analysis and Forecast, Tech. rep., Copernicus Marine Environment Monitoring Service, https://doi.org/10.5281/zenodo.4746438, 2021.

Mogensen, K., Balmaseda, M., Weaver, A., Martin, M., and Vidard, A.: NEMOVAR: A variational data assimilation system for the NEMO ocean model, ECMWF newsletter, 120, 17–22, 2009.

O'Dea, E., Furner, R., Wakelin, S., Siddorn, J., While, J., Sykes, P., King, R., Holt, J., and Hewitt, H.: The CO5 configuration of the 7 km Atlantic Margin Model: large-scale biases and sensitivity to forcing, physics options and vertical resolution, Geoscientific Model Development, 10, 2947–2969, 2017.

Palmí-Perales, F., Lindgren, F., and Gómez-Rubio, V.: Bayesian inference for case-control point pattern data in spatial epidemiology with the\texttt {inlabru} R package, arXiv preprint arXiv:2503.14954, 2025.

Raza, M., Prokopova, H., Huseynzade, S., Azimi, S., and Lafond, S.: Towards integrated digital-twins: An application framework for autonomous maritime surface vessel development, Journal of Marine Science and Engineering, 10, 1469, 2022.

Rue, H., Martino, S., and Chopin, N.: Approximate Bayesian inference for latent Gaussian models by using integrated nested Laplace approximations, Journal of the Royal Statistical Society: Series B (Statistical Methodology), 71, 319–392, https://doi.org/https://doi.org/10.1111/j.1467-9868.2008.00700.x, 2009.

Salim, M. F., Satoto, T. B. T., et al.: Predicting spatio-temporal dynamics of dengue using INLA (integrated nested laplace approximation) in Yogyakarta, Indonesia, BMC Public Health, 25, 1–17, 2025.

Satake, M., Tanaka, Y., Ishikura, Y., Oshima, Y., Naoki, H., and Yasumoto, T.: Gymnocin-B with the largest contiguous polyether rings from the red tide dinoflagellate, Karenia (formerly Gymnodinium) mikimotoi, Tetrahedron Letters, 46, 3537–3540, 2005.

Schmechtig, C., Wong, A., Maurer, T. l., Bittig, H., and Thierry, V.: Argo quality control manual for biogeochemical data, Report, https://doi.org/10.13155/40879, 2023.

Shutler, J. D., Davidson, K., Miller, P. I., Swan, S. C., Grant, M. G., and Bresnan, E.: An adaptive approach to detect high-biomass algal blooms from EO chlorophyll-a data in support of harmful algal bloom monitoring, Remote Sensing Letters, 3, 101–110, 2012.

Siddorn, J. and Furner, R.: An analytical stretching function that combines the best attributes of geopotential and terrain-following vertical coordinates, Ocean Modelling, 66, 1–13, 2013.

Silke, J., O'Beirn, F., and Cronin, M.: Karenia mikimotoi: an exceptional dinoflagellate bloom in western Irish waters, summer 2005, Marine Environment and Health Series, 21, 2005.

Skákala, J., Ford, D., Brewin, R. J., McEwan, R., Kay, S., Taylor, B., de Mora, L., and Ciavatta, S.: The assimilation of phytoplankton functional types for operational forecasting in the northwest European Shelf, Journal of Geophysical Research: Oceans, 123, 5230–5247, 2018.

Skákala, J., Ford, D. A., Bruggeman, J., Hull, T., Kaiser, J., King, R. R., Loveday, B. R., Palmer, M. R., Smyth, T. J., Williams, C. A. J., and Ciavatta, S.: Towards a multi-platform assimilative system for ocean biogeochemistry, Earth and Space Science Open Archive ESSOAr, submitted to JGR-Oceans, 2021.

Skakala, J., Awty-Carroll, K., Menon, P. P., Wang, K., and Lessin, G.: Future digital twins: emulating a highly complex marine biogeochemical model with machine learning to predict hypoxia, Frontiers in Marine Science, 10, 1058 837, 2023.

Skákala, J., Ford, D., Bruggeman, J., Hull, T., Kaiser, J., King, R. R., Loveday, B., Palmer, M. R., Smyth, T., Williams, C. A. J., and Ciavatta, S.: Towards a Multi-Platform Assimilative System for North Sea Biogeochemistry, Journal of Geophysical Research: Oceans, 126, e2020JC016 649, https://doi.org/https://doi.org/10.1029/2020JC016649, e2020JC016649 2020JC016649, 2021.

Steinmetz, F., Deschamps, P.-Y., and Ramon, D.: Atmospheric correction in presence of sun glint: application to MERIS, Opt. Express, 19, 9783–9800, https://doi.org/10.1364/OE.19.009783, 2011.

Tangen, K.: Blooms of Gyrodinium aureolum (Dinophygeae) in North European waters, accompanied by mortality in marine organisms, Sarsia, 63, 123–133, 1977.

Testor, P., de Young, B., Rudnick, D. L., Glenn, S., Hayes, D., Lee, C. M., Pattiaratchi, C., Hill, K., Heslop, E., Turpin, V., Alenius, P., Barrera, C., Barth, J. A., Beaird, N., Bécu, G., Bosse, A., Bourrin, F., Brearley, J. A., Chao, Y., Chen, S., Chiggiato, J., Coppola, L., Crout, R., Cummings, J., Curry, B., Curry, R., Davis, R., Desai, K., DiMarco, S., Edwards, C., Fielding, S., Fer, I., Frajka-Williams, E., Gildor, H., Goni, G., Gutierrez, D., Haugan, P., Hebert, D., Heiderich, J., Henson, S., Heywood, K., Hogan, P., Houpert, L., Huh, S., E. Inall, M., Ishii, M., Ito, S.-i., Itoh, S., Jan, S., Kaiser, J., Karstensen, J., Kirkpatrick, B., Klymak, J., Kohut, J., Krahmann, G., Krug, M., McClatchie, S., Marin, F., Mauri, E., Mehra, A., P. Meredith, M., Meunier, T., Miles, T., Morell, J. M., Mortier, L., Nicholson, S., O'Callaghan, J., O'Conchubhair, D., Oke, P., Pallàs-Sanz, E., Palmer, M., Park, J., Perivoliotis, L., Poulain, P.-M., Perry, R., Queste, B., Rainville, L., Rehm, E., Roughan, M., Rome, N., Ross, T., Ruiz, S., Saba, G., Schaeffer, A., Schönau, M., Schroeder, K., Shimizu, Y., Sloyan, B. M., Smeed, D., Snowden, D., Song, Y., Swart, S., Tenreiro, M., Thompson, A., Tintore, J., Todd, R. E., Toro, C., Venables, H., Wagawa, T., Waterman, S., Watlington, R. A., and Wilson, D.: OceanGliders: A Component of the Integrated GOOS, Frontiers in Marine Science, 6, https://doi.org/10.3389/fmars.2019.00422, 2019.

Tonani, M., Sykes, P., King, R. R., McConnell, N., Péquignet, A.-C., O'Dea, E., Graham, J. A., Polton, J., and Siddorn, J.: The impact of a new high-resolution ocean model on the Met Office North-West European Shelf forecasting system, Ocean Science, 15, 1133–1158, https://doi.org/10.5194/os-15-1133-2019, 2019.

Tzachor, A., Hendel, O., and Richards, C. E.: Digital twins: a stepping stone to achieve ocean sustainability?, npj Ocean Sustainability, 2, 16, 2023.

Wang, K., Menon, P. P., Veenman, J., and Bennani, S.: Safety exploration using Gaussian process classification for uncertain systems, Reliability Engineering & System Safety, 256, 110 680, 2025.

Waters, J., Lea, D. J., Martin, M. J., Mirouze, I., Weaver, A., and While, J.: Implementing a variational data assimilation system in an operational 1/4 degree global ocean model, Quarterly Journal of the Royal Meteorological Society, 141, 333–349, 2015.

Williams, C. A. J., Davis, C. E., Palmer, M. R., Sharples, J., and Mahaffey, C.: The Three Rs: Resolving Respiration Robotically in Shelf Seas, Geophysical Research Letters, 49, e2021GL096 921, https://doi.org/https://doi.org/10.1029/2021GL096921, 2022.

Williams, C. A. J., Hull, T., Kaiser, J., Mahaffey, C., Greenwood, N., Toberman, M., and Palmer, M. R.: Vertical mixing alleviates autumnal oxygen deficiency in the central North Sea, Biogeosciences, 21, 1961–1971, https://doi.org/10.5194/bg-21-1961-2024, 2024.

Wong, A. P. S., Gilson, J., and Cabanes, C.: Argo salinity: bias and uncertainty evaluation, Earth System Science Data, 15, 383–393, https://doi.org/10.5194/essd-15-383-2023, 2023.